

RSC Advances



This is an *Accepted Manuscript*, which has been through the Royal Society of Chemistry peer review process and has been accepted for publication.

Accepted Manuscripts are published online shortly after acceptance, before technical editing, formatting and proof reading. Using this free service, authors can make their results available to the community, in citable form, before we publish the edited article. This *Accepted Manuscript* will be replaced by the edited, formatted and paginated article as soon as this is available.

You can find more information about *Accepted Manuscripts* in the [Information for Authors](#).

Please note that technical editing may introduce minor changes to the text and/or graphics, which may alter content. The journal's standard [Terms & Conditions](#) and the [Ethical guidelines](#) still apply. In no event shall the Royal Society of Chemistry be held responsible for any errors or omissions in this *Accepted Manuscript* or any consequences arising from the use of any information it contains.

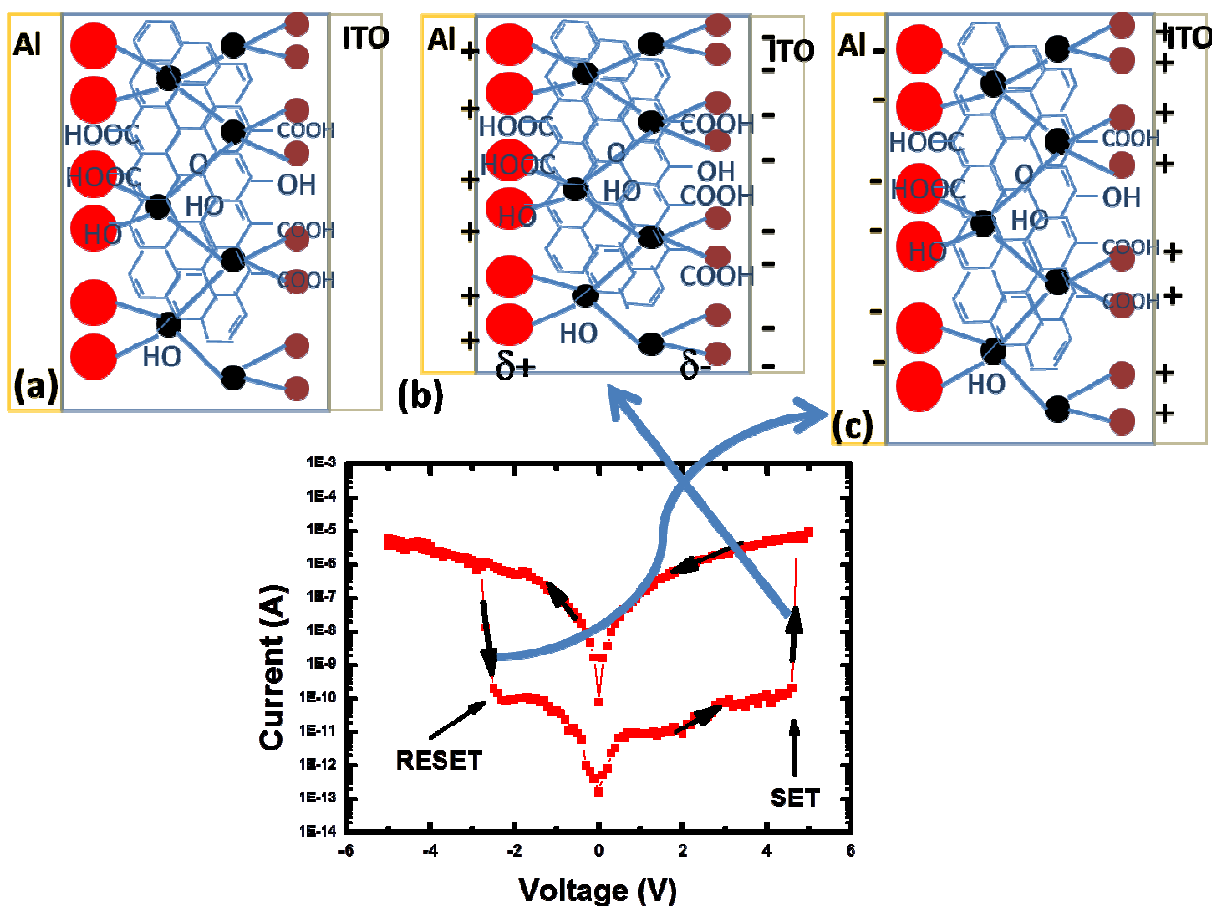
Electroforming Free High Resistance Resistive Switching of Graphene Oxide Modified Polar-PVDF

Atul Thakre^{1,2} Hitesh Borkar^{1,2}, B. P. Singh¹, Ashok Kumar^{1,2#}

¹CSIR-National Physical Laboratory, Dr. K. S. Krishnan Marg, New Delhi 110012, India

²Academy of Scientific and Innovative Research (AcSIR), CSIR-National Physical Laboratory (CSIR-NPL) Campus, Dr. K. S. Krishnan Road, New Delhi - 110012, India

A new model has been proposed for the possible high resistance resistive switching in polar beta-Polyvinylidene fluoride (β -PVDF) and graphene oxide (GO) composite. The device achieved the pre-requisite criteria of high resistance resistive switching in the range of 10-100 μ A current without electroforming.



Electroforming Free High Resistance Resistive Switching of Graphene Oxide Modified Polar-PVDF

Atul Thakre^{1,2} Hitesh Borkar^{1,2}, B.P Singh¹, Ashok Kumar^{1,2#}

¹CSIR-National Physical Laboratory, Dr. K. S. Krishnan Marg, New Delhi 110012, India

²Academy of Scientific and Innovative Research (AcSIR), CSIR-National Physical Laboratory (CSIR-NPL) Campus, Dr. K. S. Krishnan Road, New Delhi - 110012, India

Abstract:

Future nanoelectronics for nonvolatile memory elements has been looking for novel materials/devices that can switch the logic states with low power consumption, minimum heat dissipation, high-circuit density, fast switching speed, large endurance and long charge retention period. Herein, we report the novel high resistance resistive switching in polar beta-Polyvinylidene fluoride (β -PVDF) and graphene oxide (GO) composite. A high resistance switching ratio was achieved without realization of essential current-filament forming condition mainly responsible for switching the device from high to low resistance states. The β -PVDF is well known ferroelectric/piezoelectric material which changes their shape and size after application of external electric field. We proposed a model which describes that the present β -PVDF-GO composite changes their shape after application of external electric fields (E) which provides a favorable environment for the formation of current linkage path of GO in PVDF matrix. Applied positive SET electric fields (+E) switch the composite from high to low resistance state which further re-switch from low to high resistance state under negative RE-SET electric fields (-E). The positive and negative E fields are responsible for the contraction and expansion of β -PVDF, respectively, redox reactions between GO and adsorbed water, oxygen migrations, and/or metal diffusions from electrode to β -PVDF-GO matrix. The above mentioned characteristics of composites allow switching from one high resistance states to another high resistance states. The switching current lies below the range of 10-100 μ A with exceptionally high switching ratio, which meets one of the pre-requisite criteria of low power nanoelectronics memristors.

Corresponding Author: Dr. Ashok Kumar (Email: ashok553@nplindia.org)

Introduction:

Silicon based memory devices have still dominance in memory technology world due to natural integration with complementary metal-oxide semiconductor (CMOS) technology, easy to fabricate over large area, and economically viable to meet the requirements for mass production. [1,2] However with development of advance growth and fabrication technologies, till now it is possible to realize the 'Moore's Law' i.e. doubling of circuit density after 24 months. Future technology nodes i.e. less than 14 nm node technology, a novel material or process is required to meet the criteria of further downscaling in size to maintain the 'Moore's Law' for the CMOS technology with better solution of the tunneling effect and large heat dissipation due to size reduction. [3] Among the existing nonvolatile random access memories (NVRAM) such as phase-change random access memory (PRAM) [4], ferroelectric RAM (FERAM) [5], magneto-resistive RAM (MRAM) [6], and resistance random access memory (RRAM) [7,8,9,10], and memristors [11], RRAM has bright future for possible next generation non volatile memory (NVRAM) due to nano-second write and read process, high charge retention and endurance, and high ON/OFF current ratio for various logic states. However RRAM has major drawbacks that mostly it works in high current regions whereas ideally it should work in the current region down 10-100 μ A regions. [12]

PVDF polymer and its composite with GO are of special interest due to possible high resistive states, nonlinear polarization, and tunable breakdown electric (E)-field depending on the GO compositions. [13,14] Four different semicrystalline phases of PVDF, such as α -, β -, γ - and δ -phase exist in nature, among them nonpolar α -phase is most stable. [15] The polar β -PVDF has shown great technological interest where H and F atoms attached in opposite directions with the main carbon chain which develops a net dipole moment. β -PVDF is a semi-crystalline polymer that possesses high piezoelectric properties, good elasticity strength and easiness to film processing. [16] The polar β -PVDF changes their shape under applications of external electric field. The polar β -PVDF and its copolymers are one of the potential flexible polymer ferroelectric useful for FERAM, electro-caloric and flexo-electric applications. [17] Chang et al. demonstrated the resistive switching effect in ferroelectric BaTiO₃ and GO multilayer structure and found improved ON/OFF ratio of an order of 10^3 compared to basic BaTiO₃. [18] Poly (N-

Vinylecabazole)-GO composites have considered as the first report on polymer-GO based resistive switching with high ON/OFF resistance ratio, excellent retention, and bipolar resistive switching, similar effect was observed for the triphenylamine-based polyazomethine-GO composite. [19,20] The basic mechanism behind the resistive switching in above mentioned polymer composites are explained on the basis of electron transfer between GO and polymer, which in turns reduce GO under application of external applied electric field.

Fullerenes, carbon nanotubes, reduced graphene oxide and graphene-based systems have been showing exceptionally good resistive switching in cross-bar metal-insulator-metal (MIM) configuration, suggesting future materials for nonvolatile and tunable RRAM devices. [21,22,23] Graphene oxide (GO) thin films and conjugated-polymer functionalized GO films have shown robust and reproducible resistive switching. Their band-structure and electronic configurations can be easily modulated by changing the chemical functionalities attached to the surface. [24,25,26,27]. High quality GO flakes are usually prepared by chemical oxidation of natural graphite with exfoliation into individual layers. The chemical properties of these individual layers can be significantly tuned by oxidation; one can achieve the graphene with complete removal of carbon-oxygen (C-O) bond. Presence of the hydroxyl (C-OH), epoxide (C-O-C), carboxyl (COOH), and sp^2 C in the main carbon chain make the GO flakes active for oxygen migration under the application of external E-field. [28] Redox reaction and oxygen migration have been considered important mechanisms for the possible resistive switching in GO thin films and flakes. An extensive research has been carried out to understand real mechanisms for resistive switching in GO. The common consensus about the basic mechanisms are as follows; (i) gate-metal diffusion from gate to bulk GO matrix, (ii) oxygen migration/diffusions. However, till now, no tangible agreement among the researchers has been achieved. [29,30] Joeong *et al.* has provided an evidence of oxidized Al (i.e. formation of ultra Al_2O_3 thin film) near the gate (Al)-GO interface during the growth of Al by thermal evaporation, this process reduced the surface of GO film. [22] They have counter checked the role of gate-electrode by fabrication of inert metal gold (Au) electrode in which the resistive effect was absent and finally argued for the formation and destruction of local filaments in the thin insulating barrier near the interface between the top Al electrode and GO film rather than bulk GO. However the ZnO nanorods embedded GO matrix and even GO on flexible substrate illustrated the formation of bulk filaments under the application of positive E-field, contrary to the Joeong report. [13, 31, 32]. In

situ transmission x-ray microscopy studies on similar system revealed that redox reaction between GO and AlO_x and the oxygen migration are responsible for resistive switching. [33] The oxygen migration ions and related filament formation by metal cations were tested for the different top and bottom metal electrodes having different work functions with metal/GO/metal structure. It has been found that the capability of metal-oxide formation near GO-metal interface was responsible for linear and nonlinear response of GO based devices.[34,35] Apart from the MIM structure, metal-GO-semiconductor (heavily doped p-Si and p-Ge) structures were also realized with resistive switching behavior. [36] Samuele Porro et al. have reviewed the various aspects of the resistive switching in GO based memristor devices. [37]

We report a novel idea for resistive switching mechanism where basic matrix is flexible piezoelectric polymer whose dimension can be modified under application of external E-field. We will discuss filament-free current switching from one low current state to another nearby current state, however their ratio is significantly high which meet the criteria of next generation RRAM. We have critically evaluated the possible different types of conduction mechanisms involved in β -PVDF-GO composite and their theoretical fitting with the physical constants. None of them verified the ohmic behavior near the SET and RESET E-fields required for resistive switching. A model has been proposed for the oxygen migration under the external and internal (in-built) E-fields supported resistive switching.

Experimental Details:

PVDF powder was procured from Alfa Aesar India Pvt. Ltd. and Graphene Oxide was synthesized in the laboratory by conventional improved Hummer method, respectively. [38] First PVDF solution was prepared by magnetic stirring of 5 wt% PVDF powder in N, N-Dimethylformamide (DMF) solvent for 10 hrs. After realization of PVDF solution in DMF solvent, graphene oxide (in powder form) was added in the PVDF solution. The concentration of graphene oxide in the solution was kept 15 wt% w. r. t. to PVDF powder used for solution. The PVDF-GO composite solution is then again magnetic stirred for 14 hrs. Ultra-sonication is done for almost 5 hrs for homogenous mixing of GO network in the PVDF solution, later sonicated solution was filtered using the 0.5 microns filter for spin casting.

The device was fabricated on ITO coated glass substrate; latter was first cleaned by acetone than by IPA with further ultra sonication in acetone to remove any contamination on the

ITO coated surface. Spin-NXGM1 model spin coater is used for the thin film preparation. The spin coater is programmed to have a spinning speed of 2000 rpm for 30 seconds. Later, as grown films were annealed at 100°C on hot plate for 4 hrs to remove the solvent. The thin films of β -PVDF-GO composites with average thickness 120 nm were fabricated using chemical solution deposition and spin-cast techniques on ITO/coated glass substrate. Finally top aluminium electrodes having thickness around 80 nm and diameter 200 μm were deposited by thermal evaporation method using a shadow mask. All the electrical characterizations were performed on Keithley 236 source meter with the help of microprobes at ambient conditions. Voltage-current sweep was recorded for different bias voltage across top electrode through a Labview interface program. Room temperature Raman spectra were collected over wide range of wavelength using Renishaw inVia Reflex Raman spectrometer, UK (with an excitation source of 514.5 nm) with a resolution less than 1.0 cm^{-1} .

Results and Discussion:

A schematic diagram of device having Al/ β -PVDF-GO/ITO heterostructure has shown in Fig. 1 (a). Top metal (Al) electrode with large area $\sim 0.0004 \text{ cm}^2$ and almost similar distance between two electrodes was deposited by thermal evaporation technique. Various E-fields were applied from the top Al-gate to check the current response and resistive switching. The current-voltage (I-V) behavior of one of the device has illustrated in Fig. 1 (b). For the first measurement cycle, the device switches at 3.6 eV with further increase in SET E-field in next cycle which reaches upto 4.1 eV. This device gave a window of SET E-field of $\sim 0.5 \text{ V}$ as shown in Fig. 1 (b). Negative E-field was applied to RESET the device from low resistance state (LRS) to high resistance state (HRS). In the first I-V cycle, system shows RESET from LRS to HRS during the positive reverse bias E-field which may consider as discontinuities in the conduction path while decreasing the E-field form high to low potential. However after several cycles of SET and RESET process, device fails to RESET and could not provide the reproducible resistive

switching states. The above mentioned current voltage (I-V) characterization was carried out at current compliance of $I_c = 1$ mA which ruled out the current-filament formation in bulk β -PVDF-GO composite. The device failure can be seen in the context of inhomogeneous distribution of GO in PVDF matrix which is very common for the devices prepared by solution deposition techniques. The device commonly RESET during the scanning of E-field from high negative E-field towards zero.

To get the robust and reproducible resistive switching, first we have thoroughly investigated the microstructure and crystalline quality of various β -PVDF-GO composite thin films. Fig. 2(a) shows the large area optical image obtained from one of the optimized film grown in the same condition till the satisfactory level of average surface roughness ~ 15 -20 nm. The large uncertainties in the average surface roughness is mainly due to uneven distribution of GO in PVDF matrix. Later same film was examined for the surface morphology and possible grain distribution or GO flakes distribution in the PVDF matrix. Fig. 2(b) displays a smooth and homogeneous film with fine distribution of GO flakes over the large area of PVDF matrix. SEM image has ruled out the formation of grains and grain boundaries and crystalline patches in the films. Raman spectroscopy studies were carried on PVDF-GO composite to find the crystalline quality and β -PVDF phase and the possible defects stoichiometry in GO in the matrix. Left hand side inset image of Fig. 3 shows sharp intense Raman peak at 840.2 cm^{-1} suggesting that occurrence of mostly semi-crystalline β -PVDF after annealing of the spin cast film. A small amount of carbon impurities or addition of graphene or graphene related materials in any polymer matrix significantly suppressed the Raman active modes of matrix. In present investigation, major Raman modes were observed from GO in composite matrix. The G band of graphene oxide which relates the E_{2g} -vibration mode of sp^2 carbon was around 1596 cm^{-1} whereas the D band which represents the structural defects and partially disordered structures of the sp^2 domains was at 1352 cm^{-1} , their D/G intensity ratio was 0.88 which indicates the high quality GO flakes in PVDF matrix with reduction in the size of the in-plane sp^2 domains compared to the pristine graphite. [39,40] Right hand side inset image of Fig. 3 shows the 2D and D+G peaks of the GO flakes, where the D/G intensity ratio for the high frequency Raman modes was 0.94 again support the presence of good quality GO flakes in PVDF matrix. SEM

image and Raman spectra together confirm the homogeneous distribution of GO in β -PVDF matrix.

Homogeneous β -PVDF-GO composite thin film was further investigated for the current-voltage (I-V) response under various applied E-fields (Fig.4(a)). These devices also show robust resistive switching with SET E-fields from 4 to 4.8 eV, however RESET E-fields lies in the range from -1 to -2.4 V. The SET and RESET E-fields were independent of the switching cycles. For all the cases, either sweeping starts from $-E$ to $+E$ and back to $-E$ or start from 0 to $+E$ to $-E$ and back to 0 provide similar trend of SET and RESET behavior of devices. These data indicates that composite has an envelope of SET and RESET E-fields window to switch from high to low resistance states and low to high states, respectively. Fig 4 (b) shows the change in resistance (R) of the β -PVDF-GO composite under application of $+E$ field (i.e from $R \sim 2.25 \times 10^{10} \Omega$ to $R \sim 8.4 \times 10^5 \Omega$). The magnitude of resistance even after switching lies in mega ohm regions which is the basic requirement for next generation RRAM. Near the SET E-field, system shows a change in resistance of an order of 10^4 (LRS is near $M\Omega$) suggests the composite as potential candidate for high resistance switching elements. The nature of increase and decrease in resistance before and after SET E-fields, respectively never follows the ohmic law with slope nearly one, it indicates nonlinear conduction mechanism prevailed in the system. Current conduction mechanisms have been critically evaluated in subsequent section.

Various mechanisms such as oxygen diffusion, gate-metal diffusion, and electronic trapping and de-trapping of charge carriers have been employed to support the resistive switching in GO and GO-related materials. [41,42,43] Apart from the above mechanisms, we proposed a new model which might be also useful in design of novel resistive switching system. The model is based on the change in dimension under the application of external E-fields. The β -PVDF and its copolymers are well known piezoelectric/ferroelectric polymer with piezoelectric coefficient ~ 20 -30 pC/N depending on compositions and stretched conditions.[44,45] The physical nature of two major elements i.e. hydrogen and fluorine changes the shape of β -PVDF matrix under application of external E-field. Positive hydrogen ions attract the negative side of E-field and repel the positive side of E-field where as negative fluorine ions attract the positive side of E-field and repel the negative side of E-field. An application of positive E-field in the

direction of poled sample shrinks the device and hence provides a favorable path to flow the charge carriers abruptly across the hetrostructure.[46,47,48,49] Shrink condition and enough potential for the small oxygen diffusion length lead the abrupt change in the charge carriers near the SET E-fields as shown in the Fig.5 (a-c). However applications of negative E-fields separate/increase the diffusion length of oxygen ions and related vacancies and RESET the system to HRS (Fig.5(c)). It may consider that the combined piezoelectric effect of β -PVDF and oxygen diffusion makes it possible to provide high resistance resistive switching in the composite; however a careful and in-depth investigation is due using monolayer of β -PVDF and GO sheets/flakes. We cannot rule out other possible mechanisms responsible for conduction in present case since a thick layer (~ 120 nm) of β -PVDF-GO composite with limited amount of inhomogeneity has been investigated.

To better understand the mechanisms involved in the conduction process, first current-voltage (I-V) switching data were fitted for Schottky emission as shown in Fig.6 (a) in which current density can be expressed as follows:[50]

$$J_S = AT^2 \exp \left[\frac{q \left(\sqrt{\frac{qV}{4\pi\epsilon_0\epsilon_{0d}d}} - \varphi \right)}{k_B T} \right] \dots \dots \dots (1)$$

where A is Richardson constant, φ is the Schottky barrier height, k_B is Boltzmann constant, T is temperature in K, ϵ_0 is dielectric constant in vacuum, ϵ_{0d} is optical dielectric constant, q is charge carriers, V is applied potential, and d is the thickness of sample. The Fowler-Nordheim (F-N) and Schottky Emission (S-E) represent the interface mediated conduction in systems where as the F-N mechanism is mainly useful to explain the tunneling current and their mechanism under the E-field for ultra thin films. Equation 1 suggests that if Schottky emission is involve for interface mediated conduction mechanism in β -PVDF-GO composite than the $\ln J$ is proportional to $E^{1/2}$ and the slopes of the linear fitting of $\ln J$ vs. $E^{1/2}$ should provide the optical dielectric constant of β -PVDF matrix. The values of slopes (~ 0.01 to 0.1) obtained from the fitting (Fig.6 (a)) for various regions are unrealistic as compared to the real optical dielectric constant of β -PVDF. [51] These observations ruled out the possible Schottky emission mechanism involvement in the conduction process. Fig.6 (b) shows the experimental data and their fitting with bulk limited Poole-Frenkel (P-F) mechanism. [52] The physical equation related to P-F mechanism is as follows:

$$J_{PF} = cE \exp \left[\frac{q\sqrt{qV/\pi\epsilon_0\epsilon_0 d} - E_t}{k_B T} \right] \dots \dots \dots (2)$$

where c is constant, E is applied E-field, and E_t is the trap ionization energy. Current-voltage data for positive and negative biasing are fitted with the $\ln(J/E)$ vs $E^{1/2}$. Similar to S-E, the values of slopes from the linear fitting of $\ln(J/E)$ vs $E^{1/2}$ should provide the optical dielectric constant. In this situation, the magnitude of slopes of the experimental data for various applied biased E-fields regions provide an unrealistic values in the range of ~ 0.01 to 0.3 as compared to the real optical dielectric constant of β -PVDF. These values also ruled out the possible bulk limited P-F mechanism involvement in the conduction process. The experiment data and related Schottky emission and P-F mechanisms fitting suggest that negligible interface limited and bulk limited conduction process involved resistive switching, respectively.

To check the involvement of local (trapping and hopping) conduction process responsible for resistive switching, trap assisted space charge limited conduction (SCLC) process was utilized to fit with the experimental data. According to SCLC theory, trap free charge carriers follow the following physical equation; where current density linearly follows the applied E-field with slope value nearly 2. [53]

$$J_{SCLC} = \frac{9\mu_p \epsilon \theta E^2}{8d} \dots \dots \dots (3)$$

where E is bias field, ϵ is the permittivity of sample, μ_p is the mobility of charge carriers, θ is the ratio of induced free carriers to the trapped carriers. The experimental data are fitted with the $\log J$ vs E , and the value of slopes for various biased regions are given in the Fig. 7 (a & b). In most of the regions, slopes are either very near to 2 or greater than 2, as expected for the ideal SCLC mechanisms. Slope S2 and S8 represent the regions before and after the SET and RESET E-fields of resistive switching, respectively. Both regions may consider as the buffer energy region for accumulation and depletion of charge carriers before abrupt change in current. Lampert and Mark have modified the SCLC equation for the different set of charge carriers with different activation energy distributed in the various applied E-field regions. The modified equation is as follow; [54]

$$J = e\mu_p N_c \left(\frac{\epsilon}{eN_e k T_f} \right) \frac{E^{l+1}}{d^l} \dots \dots \dots (4)$$

where N_c is the effective density of states in conduction band, k_B is Boltzmann constant, N_e is the density of electrons, and T_f is the temperature parameter related to trap distribution. The

parameter $l \sim 1$ represents the shallow level traps/defects just near the bottom of conduction band which obeys the ideal SCLC J vs V^2 . The parameter $l > 1$ represents the deep level traps that follows the power law with slope greater than 2 depending on the magnitude and density of trap states [55,56]. The presence of oxygen vacancies and related defects in embedded GO in PVDF matrix may act as the trap states of electron which may be one of the reason for getting slopes greater than two. These charge carriers accelerate and deplete with various slope under applied E-field depending upon the magnitude and direction of E-field potential.

The oxygen diffusion in GO under E-field has been thoroughly investigated and well accepted mechanisms for the conduction in GO. [24] It all depends on the oxygen diffusion and their mobility on the surface of graphene plane. [41] The oxygen diffusivity is determined from the equation; $D = d^2 V_0 / [4 \exp(-\Delta E / k_B T)]$, where d is jump distance of oxygen sites, ΔE is the barrier height, V_0 is the attempt frequency. [42] According to site-on-site hopping model, decrease in barrier height and distance of oxygen sites increase the oxygen diffusivity by many folds in magnitude. Suarez et al. theoretically calculated the hopping energy height of oxygen ions after removal of one electron (under +E-field) in graphene layer and they found that their energy lies in the range of 0.7 to 0.9 eV, however during the inclusion of electron (under -E-field) it was nearly 0.15 eV which suggests the SET process is quite slower and needs high E-fields switching compared to RESET process.

In summary, a novel β -PVDF-GO composite with MIM structure has been successfully fabricated on ITO coated glass substrate and demonstrated for high resistance memristive devices. Polar β -PVDF gave an extra degree of freedom to manipulate the conducting path without electroforming during the switching from HRS to LRS and vice versa. A model has been proposed and illustrated that during the application of positive E-field, polar β -PVDF phase reduced in size due to high piezoelectric properties which in turns reduce the hopping path for the oxygen diffusion mainly responsible for the formation of conductive path. Experimental current-voltage data were fitted for several conduction mechanisms, most of them failed to explain the phenomenon, however deep level trap charge assisted modified SCLC supports the conduction mechanism. The device switches from pA to μ A current range which may consider as a major breakthrough in scale down of switching current for RRAM applications. The concept of conduction model presented in this article may be useful in fabrication of other forming-free RRAM devices

Acknowledgement:

AK acknowledges the CSIR-MIST (PSC-0111) project for their financial assistance. Atul Thakre would like to acknowledge the CSIR (JRF) to provide fellowship to carry out integrated MTech/Ph. D program. Authors would like to thank Dr. V N Ojha (Head ALSIM) for his constant encouragement and Dr. Sushil Kumar, CSIR-NPL for constant support for thermal evaporation deposition.

Figure captions:

Fig. 1 (a) Graphical representation of Al/ β -PVDF-GO/ITO heterostructure device used for electrical characterization, (b) The current-voltage (I-V) behaviors of one of the failed device in which GO is uneven distributed in PVDF matrix. The device was unable to RESET after 3rd run of I-V cycle.

Fig.2. (a) The large area optical image of β -PVDF-GO composite, (b) SEM image indicates the homogeneous distribution of GO flakes in PVDF matrix.

Fig.3. Raman spectra of β -PVDF-GO composite over wide range of frequency, left inset shows the sharp peak β -PVDF whereas the right inset illustrates the high frequency D and D+G Raman modes of GO flakes.

Fig. 4 (a) The current-voltage (I-V) characteristics of second device in which GO is evenly distributed in PVDF matrix with large number of successful SET and RESET process. (b) Resistance states, behavior and their magnitude before and after SET process.

Fig. 5 represent a model which demonstrate the shape and size of β -PVDF-GO composite under application of external E-field, (a) before SET E-field, (b) near and above the breakdown SET E-field (polar PVDF contract under +Ve E-field) , and (c) near and just below the RESET negative E-field (polar PVDF expand under -Ve E-field). I-V cycle indicates the SET and RESET process with possible piezoelectric based model.

Fig. 6 Current-voltage (I-V) switching data and their model fitting with (a) Schottky-Emission (S-E), and (b) bulk limited Poole-Frenkel (P-F) mechanism.

Fig. 7 Current-voltage (I-V) switching data and their model fitting with modified space charge limited conduction (SCLC) mechanism, (a) for SET process and (b) for RESET process.

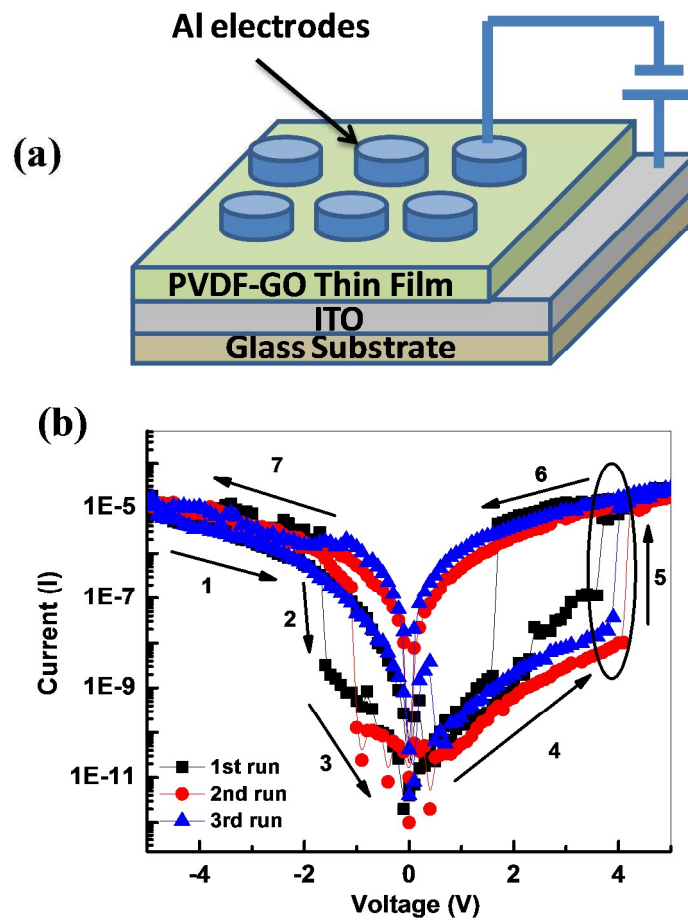


Fig.1

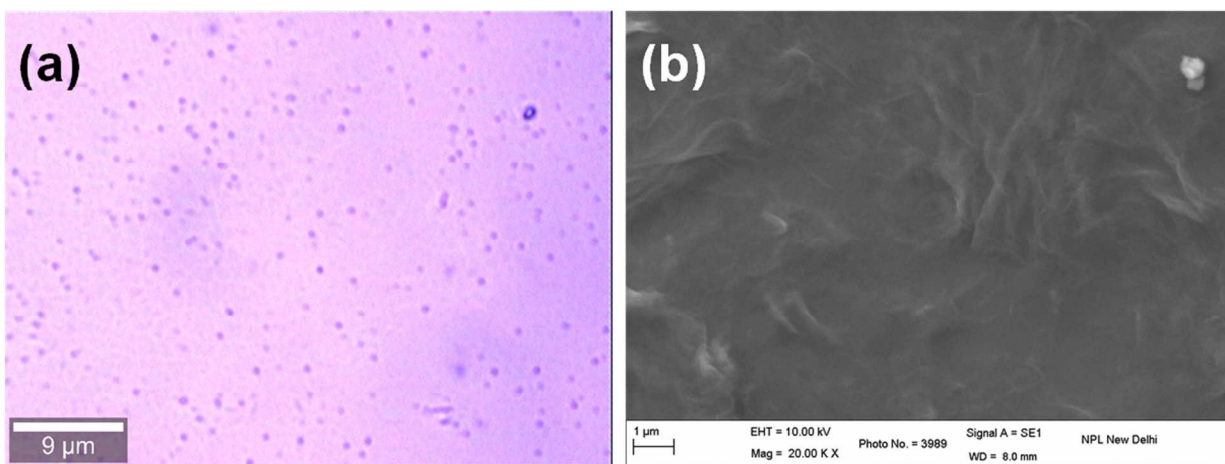


Fig.2

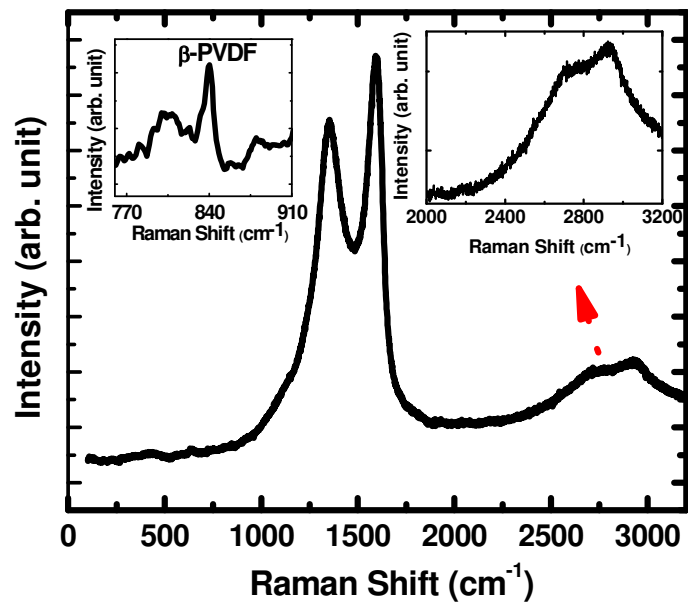


Fig.3

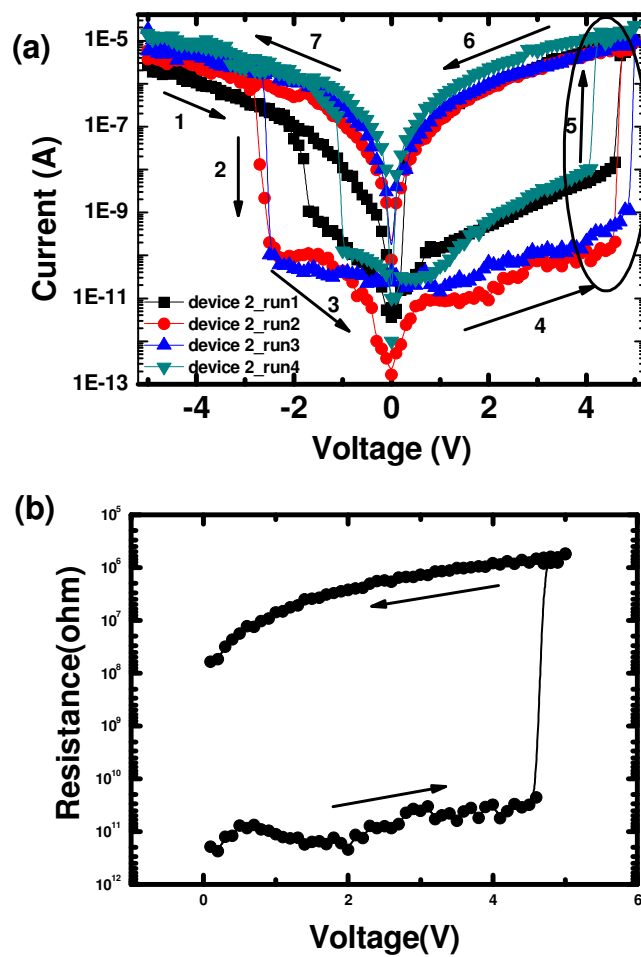


Fig.4

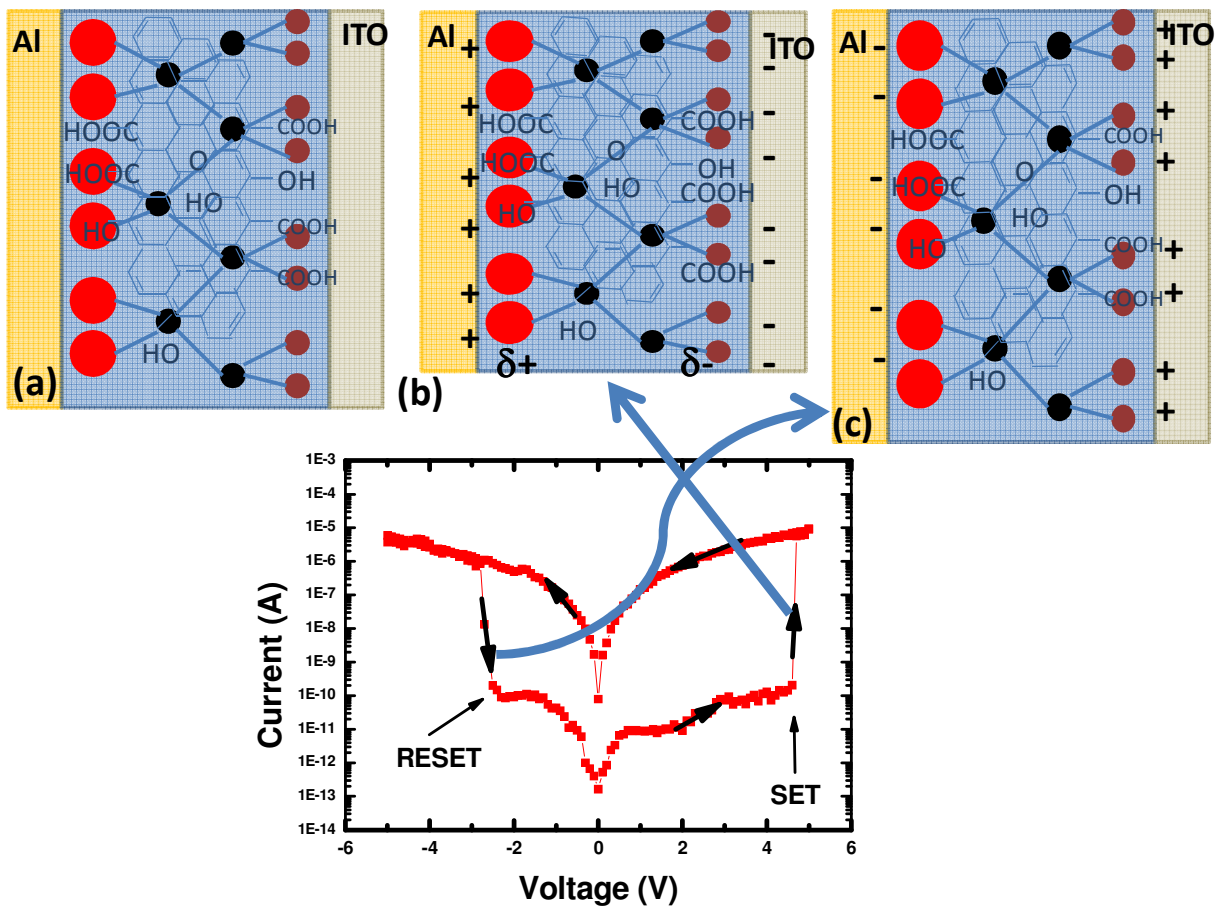


Fig.5

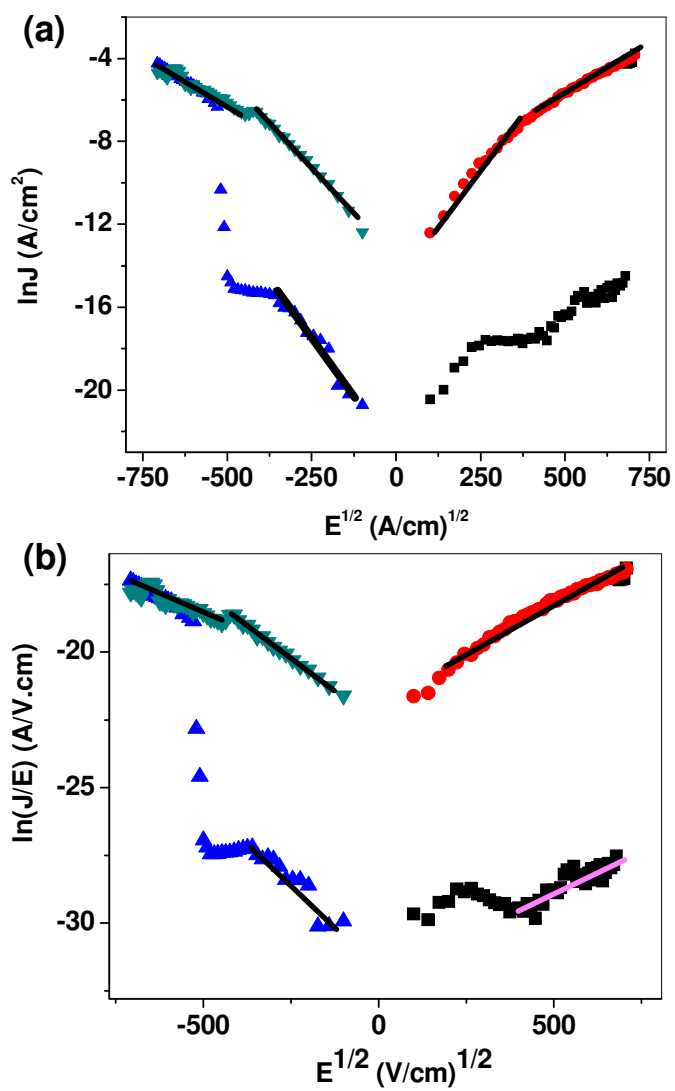


Fig.6

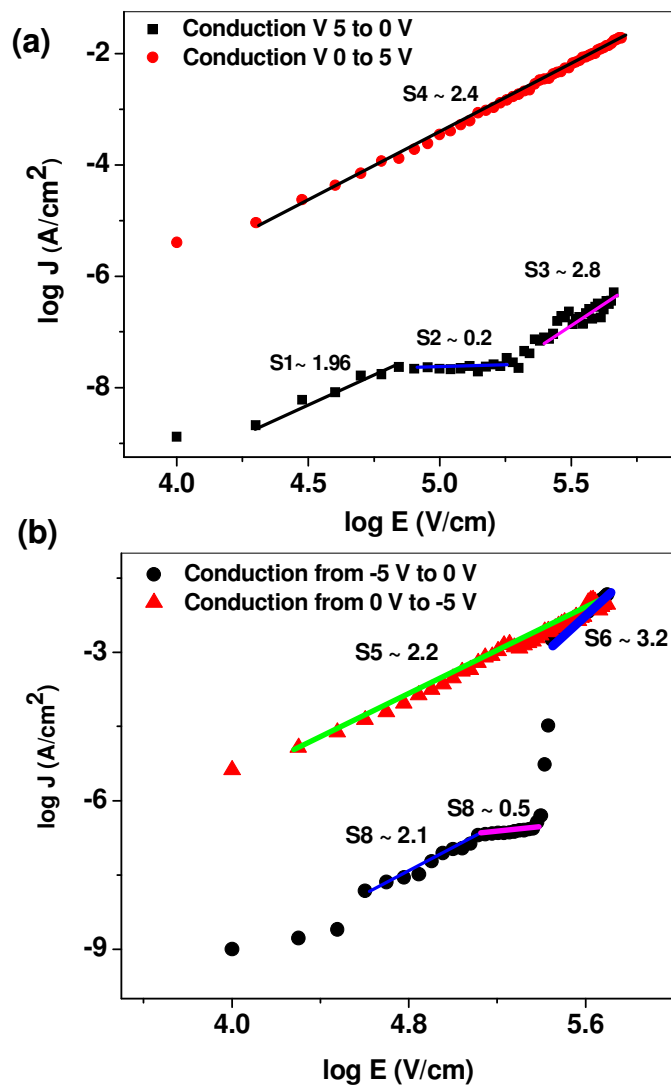


Fig.7

References:

- 1 M. J. Lee, S. Han, S. H. Jeon, B. H. Park, B. S. Kang, S. E. Ahn, K. H. Kim, C. B. Lee, C. J. Kim, I. K. Yoo, D. H. Seo, X. S. Li, J. B. Park, J. H. Lee, and Y. Park, *Nano Letters*, 2009, **9**, 1476.
- 2 S. Moller, C. Perlov, W. Jackson, C. Taussig, and S. R. Forrest, *Nature*, 2003, **426**, 166.
- 3 ITRS-The International Technology Roadmap for Semiconductors, <http://www.itrs.net/>, 2012.
- 4 H. F. Hamann, M. O'Boyle, Y. C. Martin, M. Rooks, and H. K. Wickramasinghe, *Nature Materials*, 2006, **5**, 383.
- 5 J. F. Scott, and Carlos A. Paz de Araujo, *Science*, 1989, **246**, 1400.
- 6 J. Åkerman, *Science*, 2005, **308**, 508.
- 7 R. Waser, R. Bruchhaus, and S. Menzel, *Nanoelectronics and Information Technology*, 2012, 3rd ed.
- 8 R. Waser, R. Dittmann, G. Staikov, and K. Szot, *Adv. Mater.*, 2009, **21**, 2632–2663.
- 9 Hung-Ju Yen, Hsinhan Tsai, Cheng-Yu Kuo, Wanyi Nie, Aditya D. Mohite, Gautam Gupta, Jian Wang, Jia-Hao Wu, Guey-Sheng Lioud and Hsing-Lin Wang, *J. Mater. Chem. C*, 2014, **2**, 4374
- 10 H. Borkar, A. Thakre, S. S. Kushvaha, R. P. Aloysius, A. Kumar, *RSC Advances*, 2015, **5** (44), 35046.
- 11 L. O. Chua, *IEEE Transactions on Circuit Theory*, 1971, **18**, 507.
- 12 M. J. Lee, C. B. Lee, D. Lee, S. R. Lee, M. Chang, J. H. Hur, Y. B. Kim, C. J. Kim, D. H. Seo, S. Seo, U. I. Chung, I. K. Yoo and K. Kim, *Nature Materials*, 2011, **10**, 605.
- 13 G. Khurana, P. Misra, and R. S. Katiyar, *Carbon*, 2014, **76**, 341–347.
- 14 T. Mosciatti, S. Haar, F. Liscio, A. Ciesielski, E. Orgiu and P Samorì, *ACS Nano*, 2015, **9** (3), 2357.
- 15 A. J. Lovinger, *Science*, 1983, **220**, 1115.
- 16 S. Chen, K. Yao, F. E. H. Tay, and C. L. Liow, *J. Appl. Phys.*, 2007, **102**, 104108.
- 17 R. Gregorio Jr., R. Cestari, N. C. P. S. Nociti, J. A. Mendonc, A and A. A. Lucas, *CRC Press, USA*, 1996, 2286.

-
- 18 Y. C. Chang, C. Y. Wei, and V. H. Wang, *Proc IEEE Electron Devices Solid State Circuit (EDSSC)* 2012:3–5.
- 19 G. Liu, X. Zhuang, Y. Chen, B. Zhang, J. Zhu, C. X. Zhu, K. G. Neoh and E. T. Kang, *Appl Phys Lett.*, 2009, **95**, 253301.
- 20 X. Zhuang, Y. Chen, G. Liu, P. P. Li, C. X. Zhu, E. T. Kang, K. G. Neoh, B. Zhang, J. H. Zhu, and Y. X. Li, *Adv Mater* 2010, **22**, 1731.
- 21 F. Krepl, R. Bruchhaus, P. Majewski, J. B. Phillipp, R. Symanczyk, T. Happ, C. Arndt, M. Vogt, R. Zimmermann, A. Buerke, A. P. Graham, and M. Kund, *IEEE Electron Devices Meet.*, 2008, 521–524.
- 22 H. Y. Jeong, O J. Y. Kim, J. W. Kim, J. O. Hwang, J. E. Kim, J. Y. Lee, T. H. Yoon, B. J. Cho, S. O. Kim, R. S. Ruoff and S. Y. Choi, *Nano Letters*, 2010, **10**, 4381.
- 23 C. G. Navarro, R. T. Weitz, A. M. Bittner, M. Scolari, A. Mews, M. Burghard, and K. Kern, *Nano Letters*, 2007, **7**, 3499.
- 24 C. L. He, F. Zhuge, X. F. Zhou, M. Li, G. C. Zhou, Y. W. Liu, J. Z. Wang, B. Chen, W. J. Su, Z. P. Liu, Y. H. Wu, P. Cui, and R. W. Li, *Appl. Phys. Lett.*, 2009, **95**, 232101.
- 25 C Wu, F Li, Y Zhang, T Guo, T Chen, *Appl Phys Lett* 2011, 99, 042108.
- 26 P Bhunia, E Hwang, M Min, J Lee, S Seo, S Some, and H Lee, *Chem Commun*, 2012, **48**, 913.
- 27 W. Jie, and J. Hao, *Nanoscale*, 2014, **6**, 6346.
- 28 C. Mattevi, G. Eda, S. Agnoli, S. Miller, K. A. Mkhoyan, O. Celik, D. Mastrogiovanni, G. Granozzi, E. Garfunkel, M. Chhowalla, *Adv. Funct. Mater.*, 2009, **19**, 2577.
- 29 H. S. Lee, J. A. Bain, S. Choi, and P. A. Salvador, *Appl. Phys. Lett.*, 2007, **90**, 202107.
- 30 H. Choi, H. Jung, J. Lee, J. Yoon, J. Park, D. J. Seong, W. Lee, M. Hasan, G. Y. Jung, and H. Hwang, *Nanotechnology*, 2009, **20**, 345201.
- 31 L. H. Wang, W. Yang, Q. Q. Sun, P. Zhou, H. L. Lu, S. J. Ding and D. W. Zhang, *Applied Physics Letters*, 2012, **100**, 063509.
- 32 G. Khurana, P. Misra, N. Kumar, and R. S. Katiyar, *J. Phys. Chem. C*, 2014, **118**, 21357.
- 33 H W Nho, J Y Kim, J Wang, H J Shin, S Y Choi, T H Yoon, *J Synchrotron Radiation*, 2014, **21**, 170.
- 34 F Zhuge, B Hu, C He, X Zhou, Z Liu, R W Li, *Carbon* 2011, **49**, 3796.

- 35 S K Hong, J E Kim, S O Kim, B J Cho, *Appl Phys Lett.*, 2011, 110, 044506..
- 36 M Jilani, T D Gamot, P Banerji, S Chakraborty, *Carbon*, 2013, **64**, 187.
- 37 S. Porro, E. Accornero, C. F. Pirri, C. Ricciardi, *Carbon*, 2015, **85**, 383.
- 38 T. K. Gupta, B. P. Singh, R. K. Tripathi, S. R. Dhakate, V. N. Singh, O. S. Panwar and R. B. Mathur, *RSC Adv.*, 2015, **5**, 16921.
- 39 S. Stankovich, R. D. Piner, S. T. Nguyen and R. S. Ruoff, *Carbon*, 2006, **44**, 3342.
- 40 F. Tuinstra and J. L. Koenig, *J. Chem. Phys.*, 1970, **53**, 1126.
- 41 A. M. Suarez, L. R. Radovic, E. Bar-Ziv, and J. O. Sofo, *Phys. Rev. Lett.*, 2011, **106(14)**, 146802.
- 42 G. H. Vineyard, *J. Phys. Chem. Solids*, 1957, **3(1–2)**, 121.
- 43 S. Myung, J. Park, H. Lee, K. S. Kim, and S. Hong, *Adv. Mater.*, 2010, 22(18), 2045.
- 44 H. Zhu, S. Yamamoto, J. Matsui, T. Miyashita and M. Mitsuishi, *J. Mater. Chem. C*, 2014, **2**, 6727.
- 45 Y. Fu, E.C. Harvey, M. K. Ghantasala, and M. Spinks, *Smart Mater. Struct.*, 2006, **15**, 141.
- 46 S. Bauer, *J. Appl. Phys.* 1996, **80**, 5531.
- 47 S. Lanceros-Mendez, M. V. Moreira, J. F. Mano, V. H. Schmidt and G. Bohannan, *Ferroelectrics*, 2002, **273**, 15.
- 48 R. G. Kepler, *Ferroelectric Polymers* Ch. 3 (Dekker, 1995).
- 49 J. Serrado-Nunes, V. Sencadas, A. Y. Wu, P. M. Vilarinho, and S. Lanceros-Méndez, *Materials Science Forum*, 2006, **514**, 915.
- 50 S. M. Sze, *Physics of Semiconductor Devices*, 1981, 2nd ed., Wiley, New York.
- 51 M. Abdelaziz, *J Mater Sci: Mater Electron*, 2013, **24**, 2727.
- 52 G. W. Pabst, L. W. Martin, Y.-H. Chu, and R. Ramesh, *Appl. Phys. Lett.*, 2007, **90**, 072902.
- 53 M. Dawber, K. M. Rabe, J. F. Scott, *Reviews of modern physics*, 2005, **77 (4)**, 1083.
- 54 M. A. Lampert and P. Mark, *Academic, New York*, 1970, 23.
- 55 C. J. Peng and S. B. Krupanidhi, *J. Mater. Res.*, 1995, **10**, 708.

56 N. M. Murari, R. Thomas, R. E. Melgarejo, S. P. Pavunny, and R. S. Katiyar, *Journal of Applied Physics*, 2009, **106**, 014103.